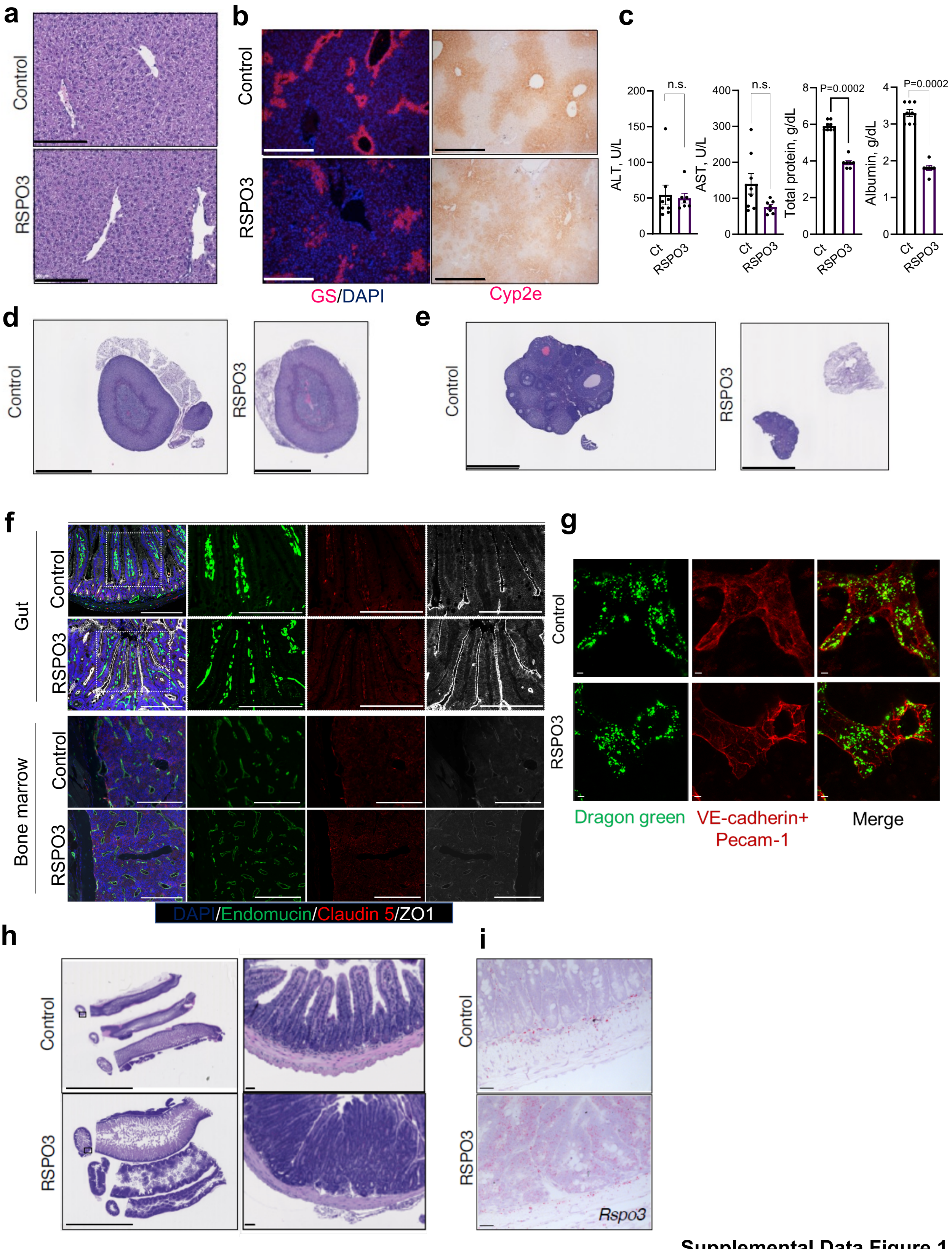

Supplemental Data Figure 1

a

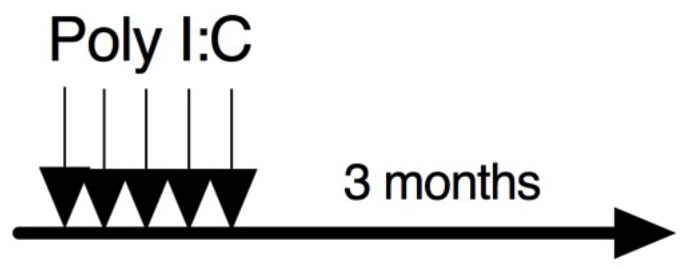

b

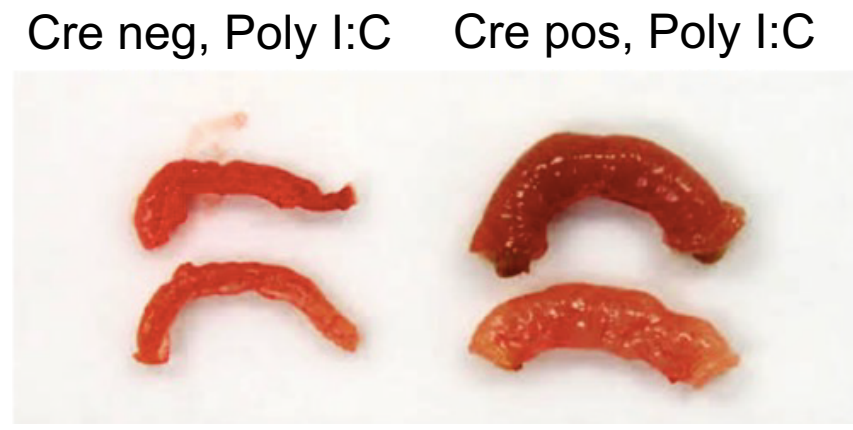

c

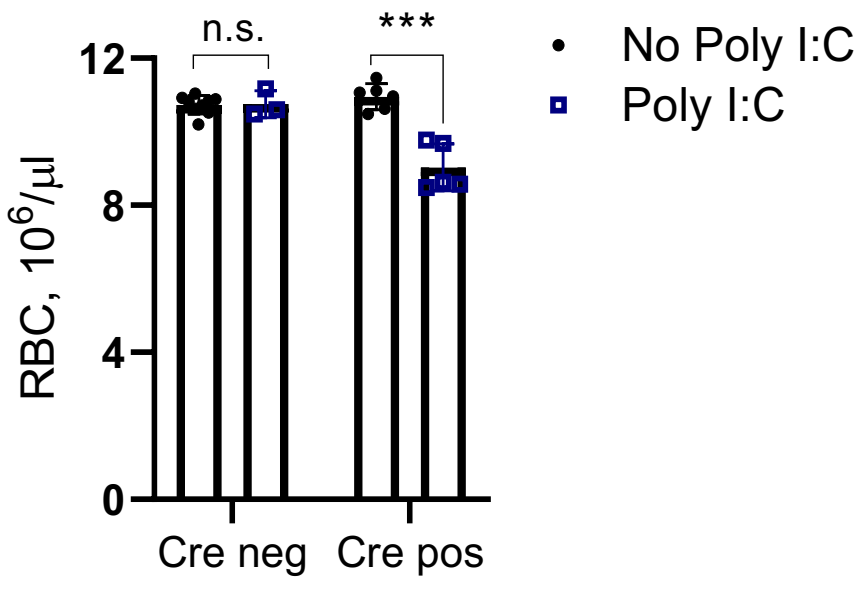

d

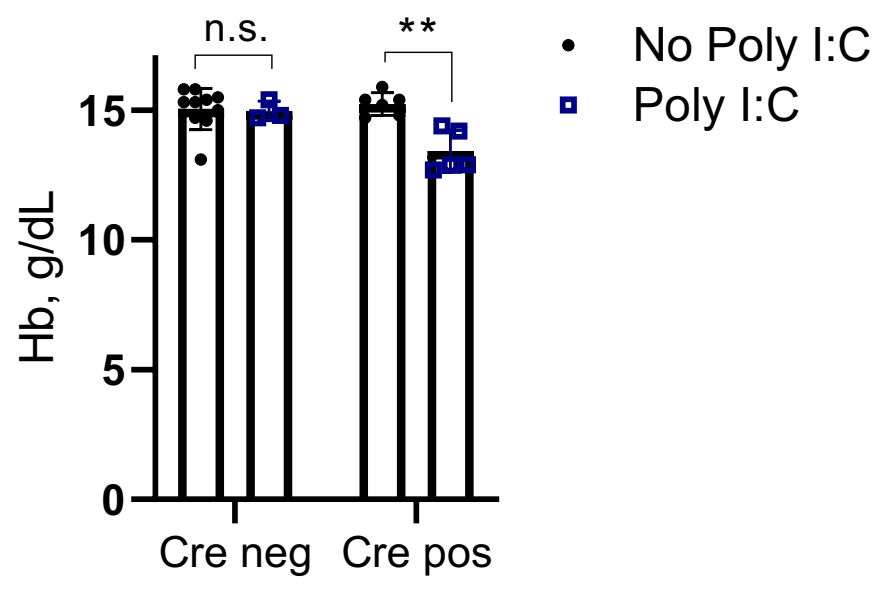

e

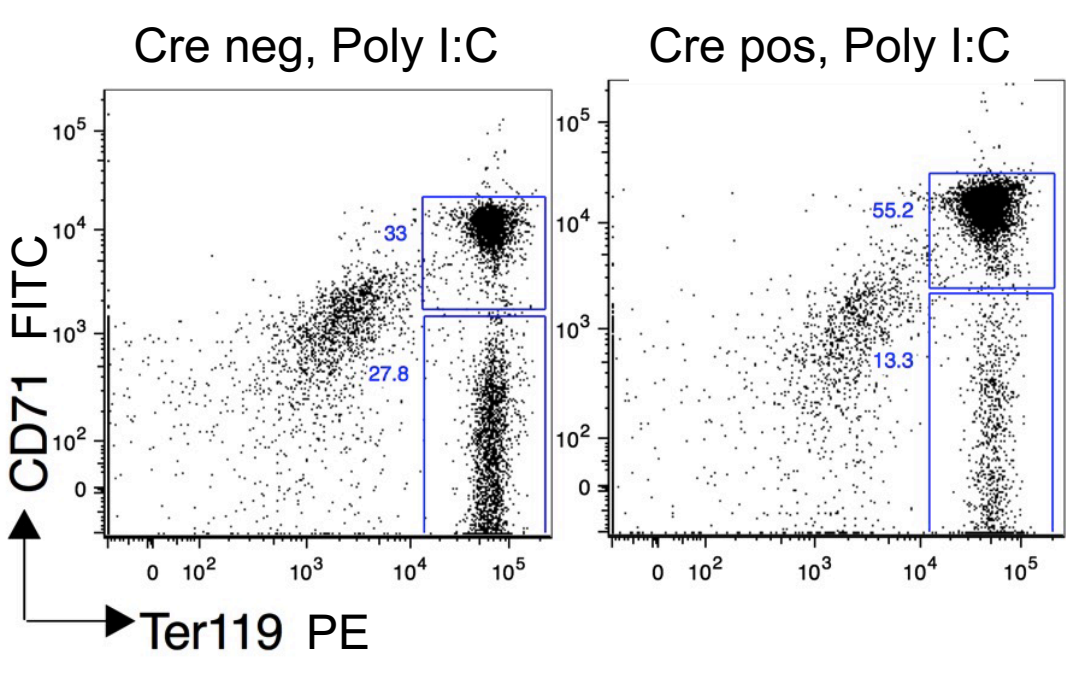

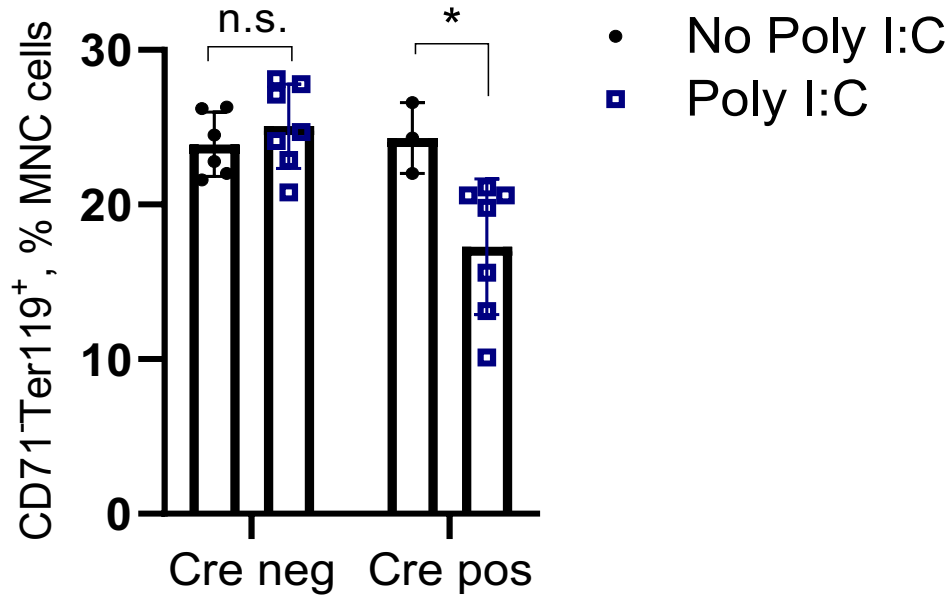

f

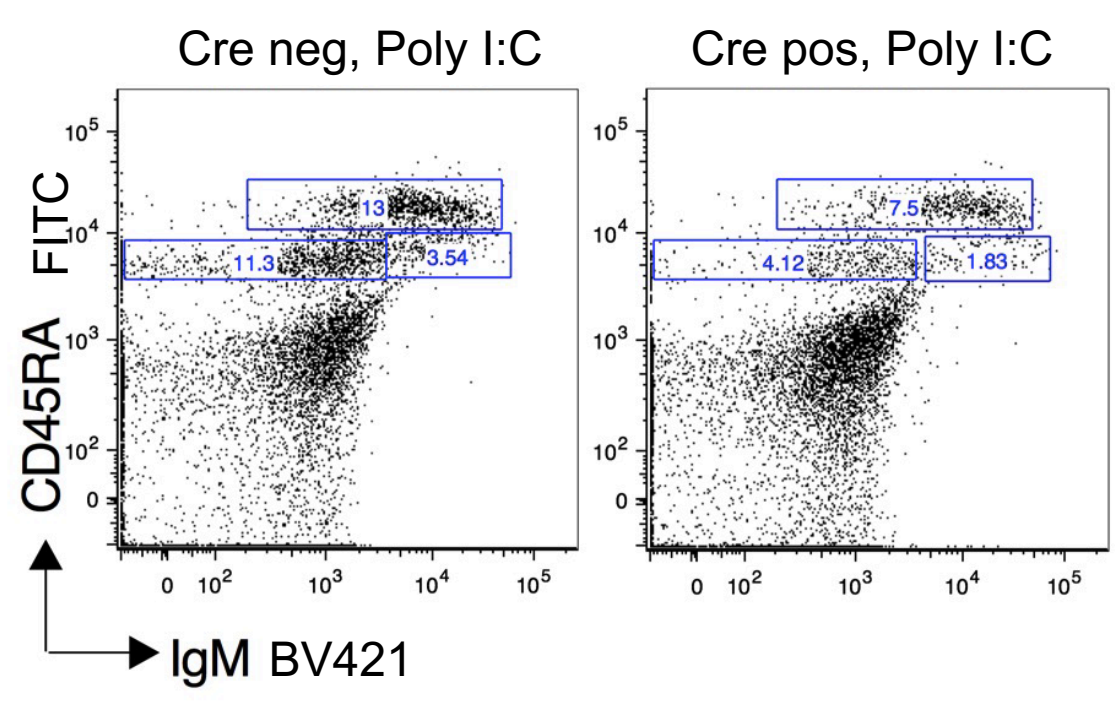

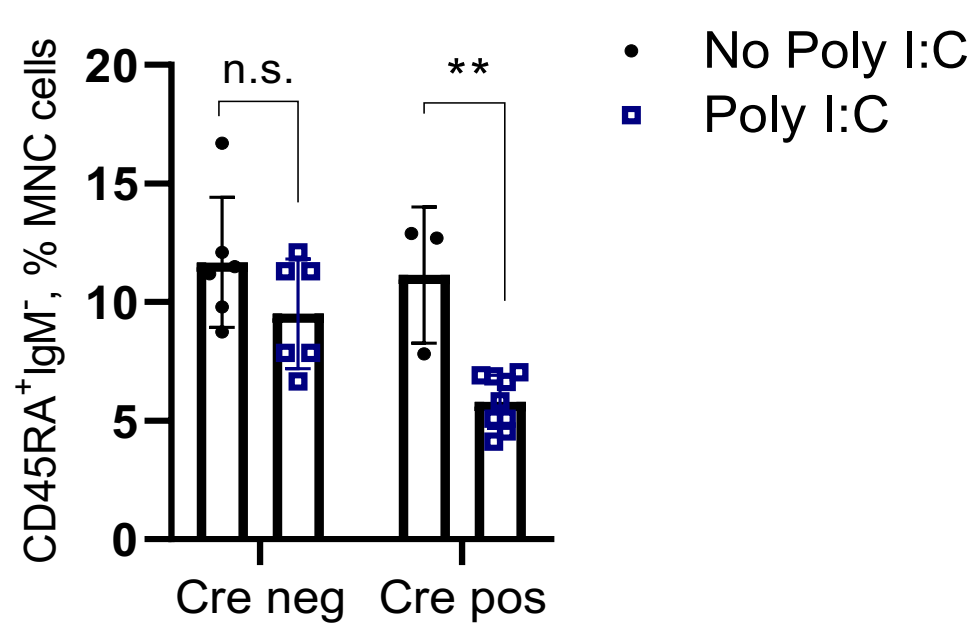

Supplemental Data Figure 2

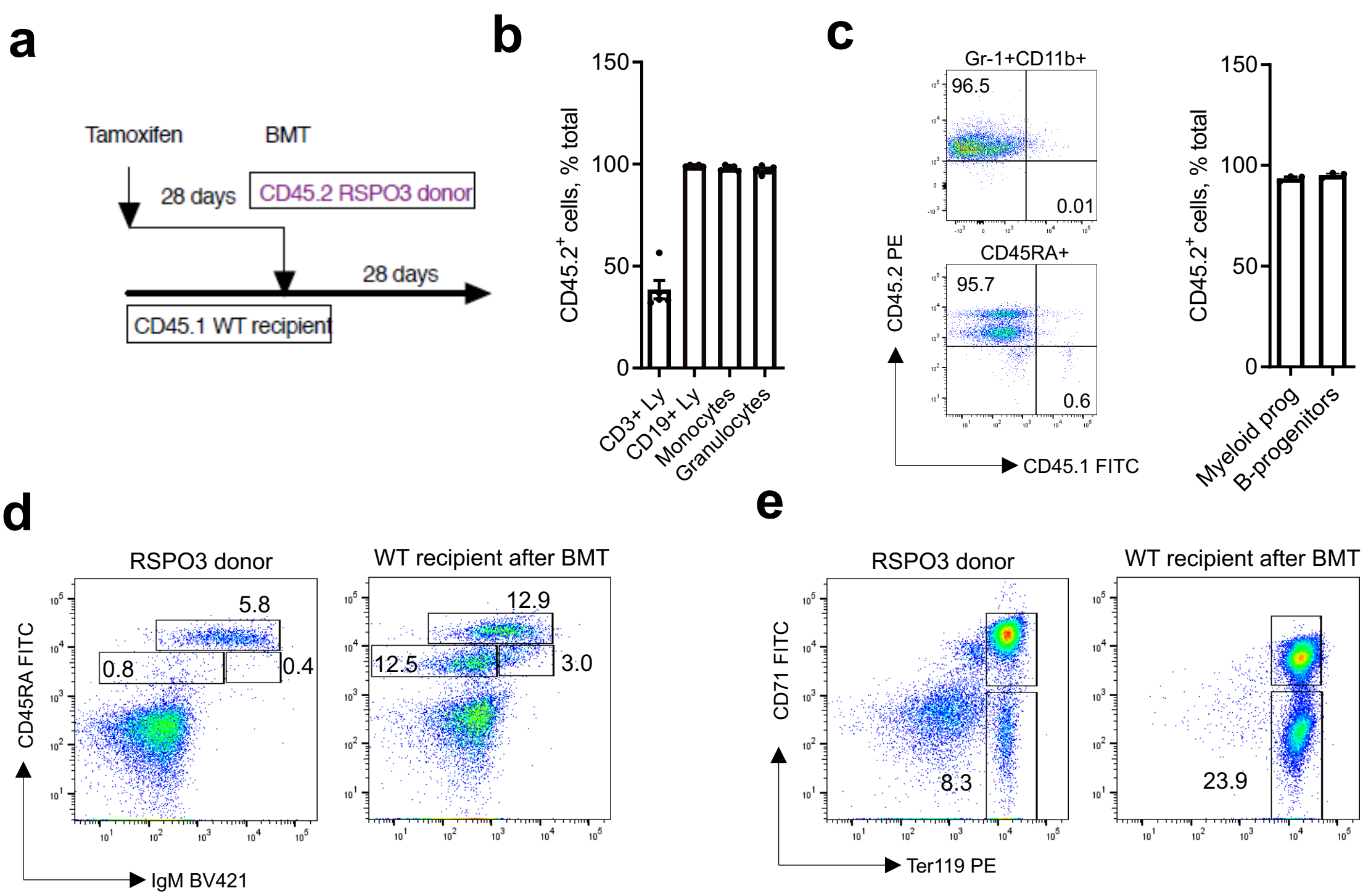

Supplemental Data Figure 3

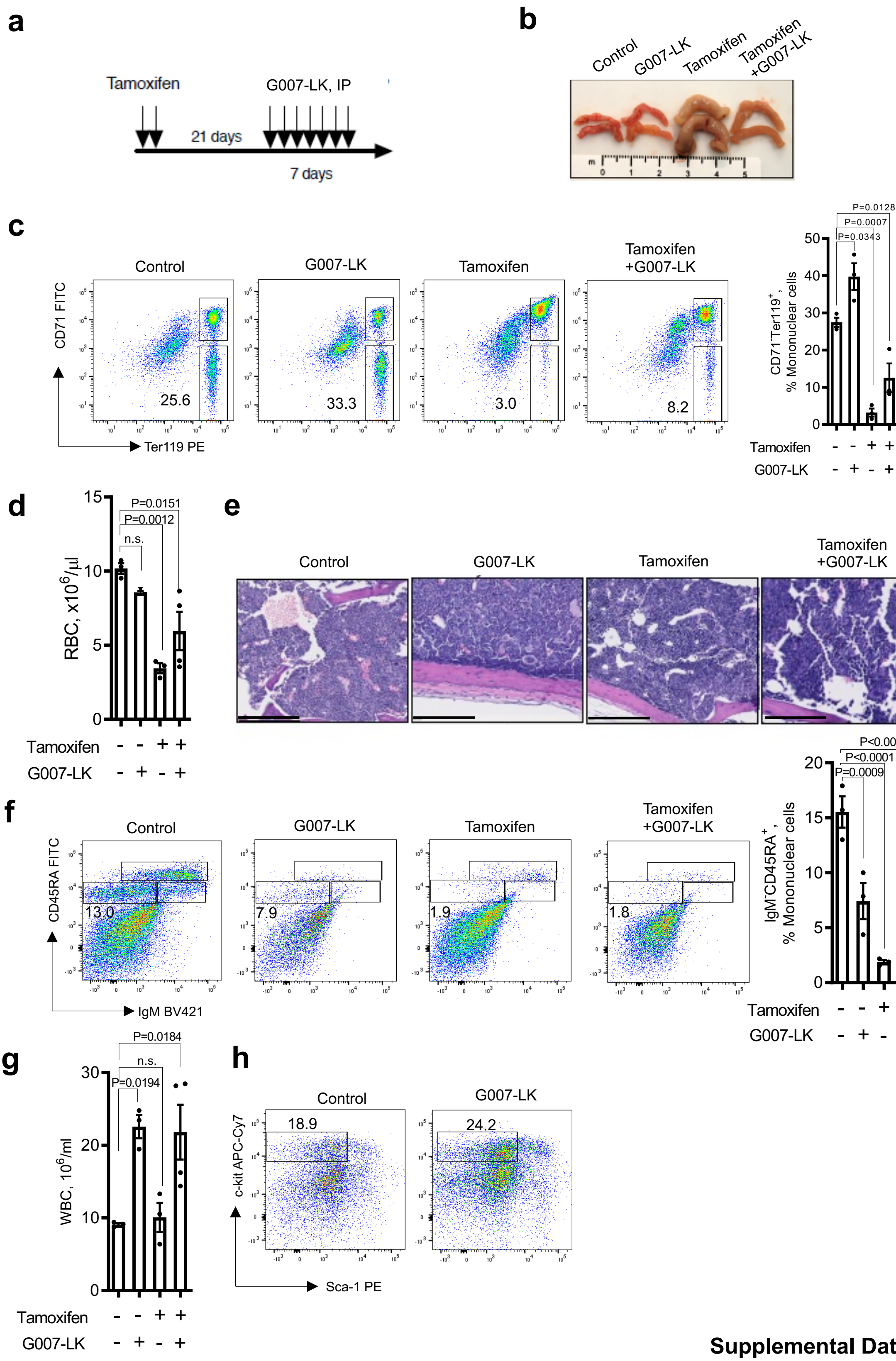

Supplemental Data Figure 4

N of donors	13
Age, years (median, range)	30 (22-39)
Gender (male/female)	7/6
Smoking (yes/no)	1/12
Medications taken within 1 week of blood collection	No: 9 Benadryl: 1 Birth control: 2 Lithium, Wellbutrin, Adderall, Latudol: 1

Supplemental Data Table 1

N of patients	29
Age, years (median, range)	74 (51-89)
IPSS-R score • Intermediate • High • Very high	 10 (34.5%) 9 (31.0%) 10 (34.5%)
WBC, 10^9/L (median, range)	2.03 (0.59-28.6)
Hemoglobin, g/L (median, range)	91 (64-112)
Platelets, 10^9/L (median, range)	42 (10-609)
Bone marrow blasts, % (median, range)	5 (0.7-17)

Supplemental Data Table 2

SUPPLEMENTAL DATA

Supplemental Data Figure 1. Characterization of a conditional RSPO3-overexpression mouse model.

a, Representative images of H&E stained liver sections from control and RSPO3 animals, n=5 per group. **b**, Representative images of liver sections from control and RSPO3 animals stained for glutamine synthetase (GS) and CYP2E1, n=3 per group. **c**, Concentration of alanine transaminase (ALT), aspartate aminotransferase (AST), total protein and albumin in serum of n=8 control and n=7 RSPO3 mice. **d**, Representative images of H&E stained adrenal gland sections from control and RSPO3 animals, n=8 per group. **e**, Representative images of H&E stained ovary sections from control and RSPO3 animals, n=8 per group. **f**, Representative immunofluorescent images of gut and bone marrow sections from control and RSPO3 animals stained for key endothelial markers, n=3 per group. Rectangles mark regions shown at higher magnification. **g**, Representative immunofluorescent images of bone marrow from control and RSPO3 animals injected with dragon green beads to assess vascular integrity, n=3 per group (VE-cadherin is CD144; Pecam-1 is CD31). **h**, Representative images of H&E stained small intestine sections from control and RSPO3 animals, n=8 per group. **i**, Representative images of ISH for *Rspo3* on small intestine sections from control and RSPO3 animals, n=3 per group. Tissues were analyzed one month after tamoxifen induction and data are represented as mean±s.e.m. Ct: control, RSPO3: tamoxifen-induced animals. n.s. not significant ($p>0.05$); two-tailed unpaired Student's t-test. Scale bars, 200μm for (**h**, right panels; **a**,**b**,**f**,**i**), 2,000μm for (**d**,**e**), 10,000μm for (**h**, left panels), 5μm for (**g**).

Supplemental Data Figure 2. Mx1.Cre driven RSPO3 overexpression recapitulates key hematopoietic phenotypes. a, schematic depicting in vivo induction regimen. **b**, gross morphology of the gut upon induction Mx1.Cre driven RSPO3 overexpression. **c**, assessment of Hb and RBC in peripheral blood of control and induced animals with various Cre status (n=3-9 mice per condition). **d**, representative FACS plots and quantification of erythroid progenitors in Mx1.Cre^{-} and Mx1.Cre^{+} mice (n=3-9 per

condition). **e**, representative FACS plots and quantification of early B-progenitors in Mx1.Cre^{-} and Mx1.Cre^{+} mice (n=3-9 per condition). Data shown as mean±s.e.m. Two-tailed unpaired Student's t-test, n.s. not significant, * p<0.05, ** p<0.01, *** p<0.001.

Supplemental Data Figure 3. Elevated RSPO3 levels are necessary to maintain the hematopoietic phenotypes. a,**f**, Schematics depicting the timeline and experimental approach of the reciprocal bone marrow transplantations (BMT). **b**, Degree of chimerism in major peripheral blood cell populations one month after transplantation of RSPO3 bone marrow into n=5 wild type (WT) recipients. **c**, Representative FACS plots and corresponding bar graph depicting the degree of chimerism in myeloid and early B-progenitors one month after transplantation of RSPO3 bone marrow into n=5 WT recipients. **d**,**e**, Representative FACS plots showing a reversal of the early B-progenitor (**d**) and erythroid progenitor (**e**) phenotypes in RSPO3 bone marrow from the same donor one month after transplantation into a WT recipient. **g**, Kaplan-Meier survival curve showing a modest survival benefit for RSPO3 animals with a WT bone marrow transplant, n=6-12 per group. **h**,**i**, Representative FACS plots showing development of the early B-progenitor (**h**) and erythroid progenitor (**i**) phenotypes in WT bone marrow from the same donor one month after transplantation into a RSPO3 recipient. Data are represented as mean±s.e.m. Difference in survival was assessed by log-rank test.

Supplemental Data Figure 4. Blocking canonical Wnt signaling does not reverse the hematopoietic phenotypes. a, Schematic depicting the tankyrase inhibitor dosing regimen. **b**, Image of representative pieces of small intestine from RSPO3 mice of each treatment group, n=3-4 per group. **c**, Representative FACS plots and corresponding bar graph quantifying erythroid progenitors in RSPO3 mice for each treatment group, n=3 per group. **d**, Absolute number of RBCs in peripheral blood from RSPO3 mice of each treatment group, n=3-4 per group. **e,** Representative images of H&E stained bone sections from RSPO3 mice of each treatment group, n=3-4 per group. **f**, Representative FACS plots and corresponding bar graph quantifying early B-progenitors in RSPO3 mice for each treatment group, n=3-4 per group. **g**, Absolute number of WBCs in peripheral blood from RSPO3 animals of each treatment group, n=3-4 per group. **h**, Representative

FACS plots showing enhanced myeloid differentiation in control animals after tankyrase inhibitor treatment, n=3-4 per group. Data are shown as mean±s.e.m. and are representative of two independent experiments. n.s. not significant (p>0.05); one-way ANOVA followed by Dunnett's test for multiple comparison. Scale bar, 500 µm.

Supplemental Data Table 1. Clinical characteristics of normal donors included in this study.

Supplemental Data Table 2. Median age and key hematological features of MDS patients included in this study. IPSS-R, Revised International Prognostic Scoring System for MDS[45].

SUPPLEMENTAL METHODS

Analyses of bone marrow, spleen, and peripheral blood. Bone marrow was collected from two femurs and two tibiae per animal and was re-suspended in IMEM with 10% FBS (both Gibco). Cell suspensions from spleens were collected by passing tissues through a 40 µm filter and re-suspending in IMEM with 10% FBS (both Gibco). No RBC lysis was performed prior to analysis of bone marrow or spleen. Peripheral blood was collected by cardiac puncture into tubes with EDTA (Vacutainer, Becton Dickinson) followed by 5min lysis with ACK Lysing Buffer (Thermo Fisher Scientific). White blood cell counts, blood differentials and platelet counts were analyzed with a Sysmex XT-2000iV hematology analyzer using mouse profile settings. Analyses of albumin, total protein, glucose, ALT and AST were performed on a BeckmanAu480 chemistry analyzer.

Tissue harvesting and processing for scRNA sequencing. Femurs, tibiae, hips and spines were dissected and cleaned from surrounding tissue. For cell sorting and flow cytometry analyses, bones were crushed with a mortar and pestle in cell suspension medium (RPMI 1640 with 2% FBC, both Gibco). The dissociated cells were passed through a 40 µm filter, spun down at 524×g for 5 min, then incubated with 5 ml ACK Lysing Buffer (Thermo Fisher Scientific) for 5 min at room temperature for RBC lysis. Neutralization of the ACK Lysing Buffer was achieved with 20ml cell suspension medium.

Cells were lineage-depleted with the Dynabeads Untouched Mouse CD4 Cells Kit (Thermo Fisher Scientific) and a custom antibody mix according to manufacturer's recommendations. For scRNA sequencing, crushed bone chips were washed four times with 10 ml of cell suspension medium, then incubated with 10 ml of digestion medium (HBSS with 1 mg/ml each of Collagenase I and Dispase, all from Gibco) for 30 min at 37ºC. The cell suspension was then passed through a 40 µm filter and the proteolysis was stopped by adding 40 ml of cell suspension medium. From this point on, cells were treated exactly the same as the dissociated bone marrow cells described above.

H&E staining & **Immunofluorescence.**

Formalin-fixed-paraffin embedded liver, gut, sternum and spleen samples were analyzed. For H&E staining slides were de-paraffinized in xylenes, re-hydrated and consecutively stained with hematoxylin (Sigma) for 5, blueing solution (Sigma) for 20 sec and eosin (Sigma) for 1 min. For IF slides were de-paraffinized in xylenes, re-hydrated, and boiled in Dako target retrieval buffer, pH6 (Dako S2369) for 25 min. Samples were first blocked with Avidin/Biotin (Vector SP-2001) following manufacturer's instructions and then for 60 min at room temperature with Dako protein-free blocking solution (Dako X0909). Primary antibody for endomucin (rat monoclonal [V.7c7.1]; Abcam ab106100 - 1:100) was applied in Dako protein-free blocking solution overnight at 4°C, followed by a 2-min Alexa 488-tyramide labeling reaction following the manufacturer's instructions (Alexa Fluor™ 488 Tyramide SuperBoost™; Invitrogen B40932). Subsequently, samples were subjected to a second antigen retrieval (as above), then blocked with Dako protein-free blocking solution (Dako X0909) for 60 min at room temperature before applying the second set of primary antibodies overnight at 4°C (rat monoclonal anti-ZO-1, clone R40.76; Sigma-Aldrich MABT11 - 1:100; rabbit polyclonal anti-Claudin 5; Abcam ab15106 - 1:100; rat monoclonal anti-CD144 (VE-cadherin), clone 11D4.1; BD 555289 - 1:100). For assessment of liver zonation, samples were processed the same way as described and primary antibodies for Gluthamine Synthetase (rabbit polyclonal; ThermoFisher Scientific, PA1-46165) and Cyp2e1 (rabbit polyclonal; Abcam ab28146) were diluted in Dako antibody diluent and exposed to samples overnight at 4 °C. Secondary antibodies (Invitrogen, Molecular Probes) for immunofluorescence staining were also diluted in

Dako antibody diluent. Secondary antibodies (goat anti-rabbit Alexa Fluor® 594; Invitrogen A-11012 - 1:500; donkey anti-rat Alexa Fluor® 647; 1:500; Jackson ImmunoResearch 712-605-153 - 1:500) diluted in Dako protein-free blocking solution were applied for 60 min at room temperature, followed by DAPI staining before mounting (ProLong Gold Antifade Mountant; Life Technologies P36930). All washes were performed using TBS-T buffer (10mM TRIS, pH 8.0, 150mM NaCl, 0.1% Tween 20). Images of entire sections were acquired on the 3D Histech Pannoramic SCAN 150 (Budapest, Hungary) with Carl Zeiss Plan-Apochromat 20x/N.A. 0.8 objective.

In vivo analysis of vascular integrity. Mice were injected with 50µl of dragon green (DG) beads (Bangs Laboratories, F502F/10597) and 130µl of antibody mix: 10µl of CD144-Alexa647 (Biolegend), 10µl of CD31-Alexa647 (Biolegend) and 110 µl of PBS (Gibco) 10 min before euthanization, and were immediately perfused with 10ml PBS by cardiac puncture before organ collection. Mouse organs were fixed at 4°C in 4%PFA for 2 hours, followed by incubation in 15% sucrose overnight, and 30% sucrose for 2 hours; fixed samples were snap frozen in OCT (Tissue-Tek) and kept at −80 °C until sectioning. Frozen samples were sectioned (7 µm) on Cryostat equipped with the Cryojane tape transfer system and tungsten blades (Leica Microsystems). Sections were washed in PBS for 3 times and imaged using an upright SP8 Leica microscope with water immersion.

Bone marrow transplantation assay. Bone marrow from $CD45.1^+$ and $CD45.2^+$ mice was collected from femurs and tibia as described. For non-competitive transplantation experiments $2x10^5$ of total bone marrow cells were injected into the tail vein of lethally irradiated (2 doses of 550 rads) mice. Relative engraftment of $CD45.2^+$ or $CD45.1^+$ donor cells was assessed in peripheral blood leukocytes and bone marrow progenitors by flow cytometry as described at 4 weeks after transplantation.

Confirmation of β-catenin deletion using genomic PCR

To confirm the specific deletion of β-catenin, mice were bled 4 weeks after the last treatment with polyI:C, red blood cells were lysed using ACK (Gibco) and $CD45^+$ cells were sorted on the FACSAria Fusion (BD). DNA was extracted using the Puregene Kit

(Qiagen) with RNAse digestion (Qiagen) following manufacturer's instruction. DNA concentration was determined using the NanoDrop (Thermo Fisher Scientific). PCR genotyping was performed using the primers ACT GCC TTT GTT CTC TTC CCT TCT G (β-catenin lox 5'), CAG CCA AGG AGA GCA GGT GAG G (β-catenin lox 3') and CAG ACA GAC AGC ACC TTC AGC ACT C (β-catenin lox_del). PCR products were analyzed on a 2% agarose gel. Gel images were taken on an AlphaImager (Protein Simple).

RNA-sequencing and data analysis. Bulk RNA-sequencing (RNA-seq) was performed on tissue from the small intestine and B- and erythroid progenitors isolated as described. Libraries were prepared with the TruSeq RNA Sample Preparation kit (Illumina, CA) and were sequenced on Illumina HiSeq 2500 sequencers to obtain on average 34 million 50-bp single-end reads per sample. RNA-seq reads were first aligned to ribosomal RNA sequences to remove ribosomal reads. The remaining reads were aligned to the mouse reference genome (NCBI Build 38) using GSNAP version[64] 2013-10-10, allowing a maximum of two mismatches per 50-base sequence (parameters: -M 2 -n 10 -B 2 -i 1 -N 1 -w 200000 -E 1–pairmax-rna = 200000–clip-overlap). Transcript annotation was based on the RefSeq database (NCBI Annotation Release 104). To quantify gene expression levels, the number of reads mapped to the exons of each RefSeq gene was calculated. Read counts were scaled by library size, quantile normalized and precision weights were calculated using the voom R package[65]. Subsequently, differential expression analysis on the normalized count data was performed using the limma R package[66] by contrasting RSPO3 overexpressing samples with control samples, respectively. Gene expression was considered significantly different across groups if we observed an |log2-fold change| ≥ 1 (estimated from the model coefficients) associated with an FDR adjusted P-value ≤ 0.05. In addition, gene expression was obtained in the form of normalized reads per kilobase gene model per million total reads (nRPKM) as described[67].

Single-cell RNA sequencing and data analysis. For single-cell RNA sequencing (scRNA seq) using the 10x Genomics platform, bone and bone marrow cells were processed as described. In addition to FACS markers, cells were stained with a DNA dye

(Vybrant™ DyeCycle™Violet, Thermo Fisher Scientific) to exclude debris and ensure that only cells are sorted for droplet based scRNA-seq. For this purpose, $3x10^6$ cells were incubated for 30 min at 37 ºC in 1ml of cell suspension medium supplemented with 2.5µl Vybrant dye. Afterwards, cells were placed on ice and a total of $1.0\text{-}1.5x10^4$ events per condition were sorted immediately into 15µl PBS containing 2% FBS. Cell numbers were confirmed with LUNA™ Automated Cell Counter (Logos Biosystems) and 33.8 µl of cell suspension was used as input without further dilution or processing, with final concentrations around 100-200 cells/µl. Reverse transcription and library construction were carried out with the Chromium Single Cell 3' Reagent v2 protocol (10x Genomics, Pleasanton, CA) according to manufacturer's recommendations. Total cDNA synthesis required 14 amplification cycles, with final cDNA yields ranging from approximately 2 to 10 ng/µl. 10x Genomics libraries were sequenced on an Illumina Next-Seq500, with read length 26+58 or 26+98. Raw sequencing data were processed using the CellRanger pipeline (10x Genomics). Unique molecular identifier (UMI) count tables were loaded into R and further processed using the Seurat R package[68]. We removed all cells with less than 500 distinct genes observed, or cells with more than 5% UMI stemming from mitochondrial genes, and the first 16 PCs were selected as input for clustering and t-SNE, based on manual inspection of a PC variance plot ("PC elbow plot"). Clustering was performed using the default method from the Seurat package, with resolution parameter set to 5. While lower resolution parameters caused biologically distinct groups with a low number of cells to be merged into single cluster, this relatively large parameters resulted in groups with a high number of cells to be split into an undesirable number of subgroups. We therefore computer the mean scaled gene expression values for each cluster and performed hierarchical clustering of the means using a correlation distance. Clusters with correlations of greater 0.8 were then merged together to result in the final clusters displayed in **Figure 2a**. Marker genes for each population were identified using the FindMarkersAll function and ROC-based test statistics.

ADDITIONAL REFERENCES

64. Wu TD, Nacu S. Fast and SNP-tolerant detection of complex variants in short reads. *Bioinformatics*. 2010;26(7):873-81.

65. Law CW, Chen Y, Shi W, Smyth G. K. voom: precision weights unlock linear model analysis tools for RNA-seq read counts. *Genome Biol.* 2014;15:R29.
66. Ritchie ME, Phipson D, Wu D, et al. limma powers differential expression analyses for RNA-sequencing and microarray studies. *Nucleic Acids Res.* 2015;43:e47.
67. Srinivasan K, Friedman BA, Larson JL, et al. Untangling the brain's neuroinflammatory and neurodegenerative transcriptional responses. *Nat Commun.* 2016;7: 11295.
68. Butler A, Hoffman P, Smibert P, Papalexi E, Satija R. Integrating single-cell transcriptomic data across different conditions, technologies and species. *Nat Biotechnol*. 2016;36:411-420.